

1

2 Negative selection on a *SOD1* mutation limits canine degenerative
3 myelopathy while avoiding inbreeding

4

5 Hisashi Ukawa^a, Noriyoshi Akiyama^{a,b}, Fumiko Yamamoto^a, Ken Ohashi^a, Genki Ishihara^b, Yuki
6 Matsumoto^{*a,b,c}

7

8 ^aGenetic Testing Section, Anicom Pafe Inc., Kanagawa, Japan

9 ^bResearch and Development Section, Anicom Specialty Medical Institute Inc., Kanagawa, Japan

10 ^cData Science Center, Azabu University, Kanagawa, Japan

11

12 *Corresponding author: Yuki Matsumoto

13 Email: y-matsumoto@azabu-u.ac.jp

14

15 **Abstract**

16 Several hundred disease-causing mutations are currently known in domestic dogs. Breeding
17 management is therefore required to minimize their spread. Recently, genetic methods such as
18 direct-to-consumer testing have gained popularity; however, their effects on dog populations are
19 unclear. Here, we aimed to evaluate the influence of genetic testing on the frequency of
20 mutations responsible for canine degenerative myelopathy (DM) and assess the changes in the
21 genetic structure of a Pembroke Welsh corgi population from Japan. Genetic testing of 5,512
22 dogs for the causative mutation in superoxide dismutase 1 (*SOD1*) (c.118G>A (p.E40K))
23 uncovered a recent decrease in frequency, plummeting from 14.5% (95/657) in 2019 to 2.9%
24 (24/820) in 2022. Weir and Cockerham population differentiation (F_{ST}) and simulation-based
25 genome-wide single-nucleotide polymorphism (SNP) analysis of 117 selected dogs revealed 143
26 candidate SNPs for selection. The SNP with the highest F_{ST} value was located in the intron of
27 *SOD1* adjacent to the c.118G>A mutation, supporting a strong selection signature on *SOD1*.
28 Further genome-wide SNP analyses revealed no obvious changes in inbreeding levels and
29 genetic diversity between the 2019 and 2022 populations. Our study highlights that genetic
30 testing can help inform improved mating choices in breeding programs to reduce the frequency of
31 risk variants and avoid inbreeding. This combined strategy could decrease the genetic risk of
32 canine DM, a fatal disease, within only a few years.

33

34 **Keywords**

35 genetic testing, canine degenerative myelopathy, artificial selection, effective population size,
36 inbreeding

37

38 **Significance statement**

39 Genetic breeding methods using direct-to-consumer testing have gained popularity, but their
40 effects on dog populations remain unclear. In this study, the effect of direct-to-consumer genetic
41 testing on *SOD1* mutation, the causative element of canine degenerative myelopathy, in a
42 domestic dog population (Pembroke Welsh corgi) from Japan was investigated. Our analyses
43 revealed that since the expansion of genetic testing in 2019, breeders used these tests to
44 artificially select against the *SOD1* mutation, considerably decreasing its occurrence in the corgi
45 population within only a few years (2019 versus 2022). Our study makes a substantial
46 contribution to existing literature by providing empirical evidence that direct-to-consumer genetic
47 testing can have rapid influence on pet genetics, noticeable in a span of 2–3 years.

48

49 **Introduction**

50

51 Genetic testing for disease-causing mutations in companion animals is increasingly performed by
52 veterinarians for diagnosis, by breeders to reduce the incidence of inherited disease, and even by
53 pet owners to determine the genetic background of their pets (Moses et al. 2018). Genetic tests
54 employed by pet owners are termed direct-to-consumer (DTC) testing and can be broadly
55 classified into two categories: 1) detection of specific mutations using sequencing or probes and
56 2) high-throughput genotyping using genome-wide marker sets designed to detect multiple
57 mutations simultaneously. In addition to their convenience, these DTC tests also yield data with
58 substantial implications for genetic research. For example, a recent study using DTC test
59 samples revealed breed-specific genetic mutations associated with hypertrophic cardiomyopathy
60 in several cat breeds (Akiyama et al. 2023). Another study, employing over 10,000 DTC samples,
61 determined the allele frequencies of 12 genes associated with canine coat color and the physical
62 characteristics of different dog lineages (Dreger et al. 2019). The results indicated that random
63 mating between certain dog breeds can produce unexpected phenotypes, including embryonic
64 lethality (Dreger et al. 2019). Moreover, although at least 775 disease-associated mutations are

65 already known in dogs (Rokhsar et al. 2021), a recent genome-wide association study using DTC
66 genetic testing data revealed a novel and unexpected in-frame deletion that causes deafness in
67 Rhodesian ridgebacks (Kawakami et al. 2022). Thus, the widespread adoption of animal genetic
68 testing greatly benefits genetic studies.

69 Genetic testing for adult dogs was introduced in Japan in 2017, followed by testing for
70 puppies in 2019. The results of such widespread testing could affect dog populations by
71 preventing carriers from breeding, thus limiting the number of genetically affected animals.
72 However, the actual effect of widespread testing on mutation frequency remains unclear. In
73 addition, while breeding to avoid mutant alleles could affect the genetic structure and inbreeding
74 levels in dog populations, only a few studies have investigated this possibility.

75 Since the initial report of the draft genome of domestic dogs in 2005 (Lindblad-Toh et al.
76 2005), significant advancements have been made in canine genetic research. Inbreeding and
77 genetic structures have been evaluated at the population level based on microsatellite and
78 genome-wide single-nucleotide polymorphism (SNP) analyses (Boyko et al. 2009; Mellanby et al.
79 2013; Dreger et al. 2016; Chu et al. 2019). Accordingly, genome-wide SNP analyses can be
80 employed to evaluate the influence of expanded DTC genetic testing on genetic structure in dog
81 populations.

82 Canine degenerative myelopathy (DM) is a fatal neurodegenerative disease prevalent in
83 several dog breeds, including the Pembroke Welsh corgi (PWC), German shepherd, and boxer
84 (Neeves and Granger 2015). The c.118G>A mutation in the superoxide dismutase 1 (*SOD1*)
85 gene (p.E40K on chromosome 31; 26,540,342 bp, based on CanFam 3.1) is reportedly a
86 causative factor of DM in PWCs (Awano et al. 2009). *SOD1* is one of the two antioxidant
87 isozymes responsible for specifically eliminating free superoxide radicals in mammals. The
88 homozygous A allele mutation is strongly associated with DM onset (Awano et al. 2009; Chang et
89 al. 2013; Zeng et al. 2014), indicating that it is an autosomal recessive variant. The mutant
90 homozygous A allele is fairly common in PWCs and is not geographically restricted (e.g., 48.4%

91 or 59/122 in Japan (Chang et al. 2013) and 83% or 14/21 in Mexico (Ayala-Valdovinos and
92 Gomez-Fernandez 2018)).

93 In this study, we evaluated the allelic frequency of *SOD1*: c.118G>A (p.E40K) mutation in
94 a population of over 5,500 PWCs from Japan, analyzing DTC genetic testing data across three
95 years (2019–2022). PWCs born from 2012 to 2022 were included in this dataset, allowing us to
96 examine the impact of genetic testing on the PWC population for both adult dogs and puppies
97 that were introduced in 2017 and 2019, respectively. We also performed a genome-wide analysis
98 to detect and compare selection signatures between the populations in 2019 and 2022. Finally,
99 we assessed inbreeding and population structures based on genome-wide SNPs to determine
100 the effects of genetic testing on dog breeding. The findings of this study could provide valuable
101 insights into how widespread genetic testing controls the spread of genetic disorders among
102 dogs.

103

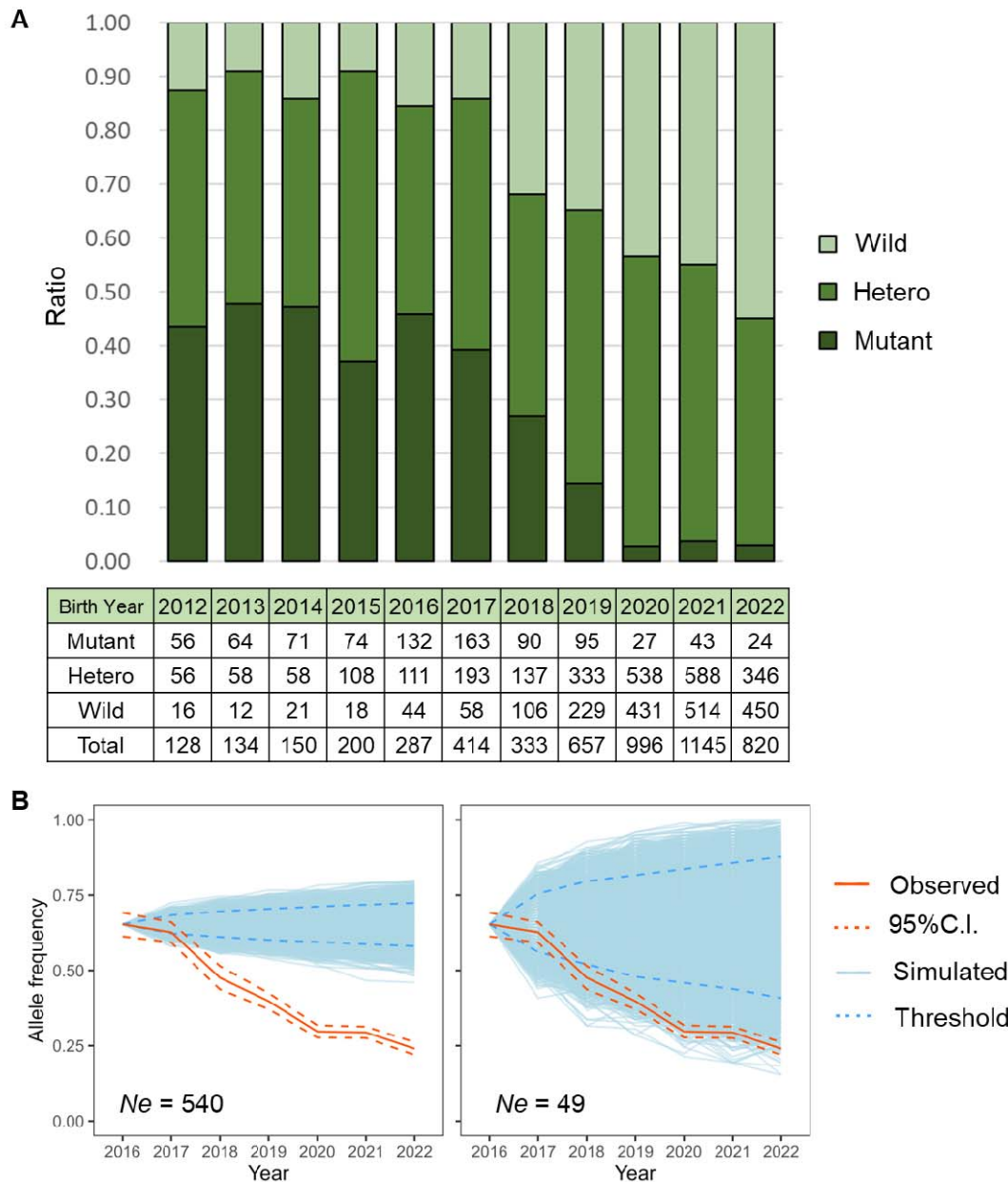
104

105 **Results**

106

107 ***Allele frequencies of the SOD1: c.118G>A variant***

108 We examined the distribution of *SOD1*: c.118G>A by birth year in 5,512 PWCs (Fig. 1A).
109 Most PWCs born between 2012 and 2017 were homozygous for the mutant allele (Mutant) or
110 heterozygous (Hetero), whereas homozygous wild-type (Wild) exhibited the lowest frequency
111 (9.0% or 12/134 in 2013 to 15.3% or 44/287 in 2016). With the initiation of genetic testing for adult
112 dogs in 2017, the frequency of the Mutant decreased from 39.4% (163/414) in 2017 to 2.9%
113 (24/820) in 2022.



114

115 **Figure 1. Trends in diploid genotype and allele frequencies of the SOD1: c.118G>A**
116 **mutation.**

117 A: Diploid genotype frequencies of the *SOD1*: c.118G>A mutation from 2012 to 2022. The ratio of
118 allele frequency is based on the birth year of tested dogs. The lower chart shows the number of
119 tested dogs divided by each diploid genotype. B: Real and simulated allele frequencies of the
120 *SOD1*: c.118G>A mutation for six years after 2016 based on two models: large ($Ne = 540$, left)

121 and small ($N_e = 49$, right) models (see Methods for details). The orange line indicates the
122 observed allele frequency, and the dashed orange lines indicate 95 percentile confidence
123 intervals. The light-blue lines indicate 10,000 simulated allele frequencies starting from 2016, and
124 the dashed blue lines indicate 95 percentile thresholds.

125

126 Since 2019, when genetic testing in puppies began, the ratio of each diploid genotype
127 has changed significantly, considering the ratios observed in 2022 (Fisher's exact test, $P =$
128 0.001). Specifically, the proportion of Mutants decreased from 14.5% (95/657) in 2019 to 2.9%
129 (24/820) in 2022.

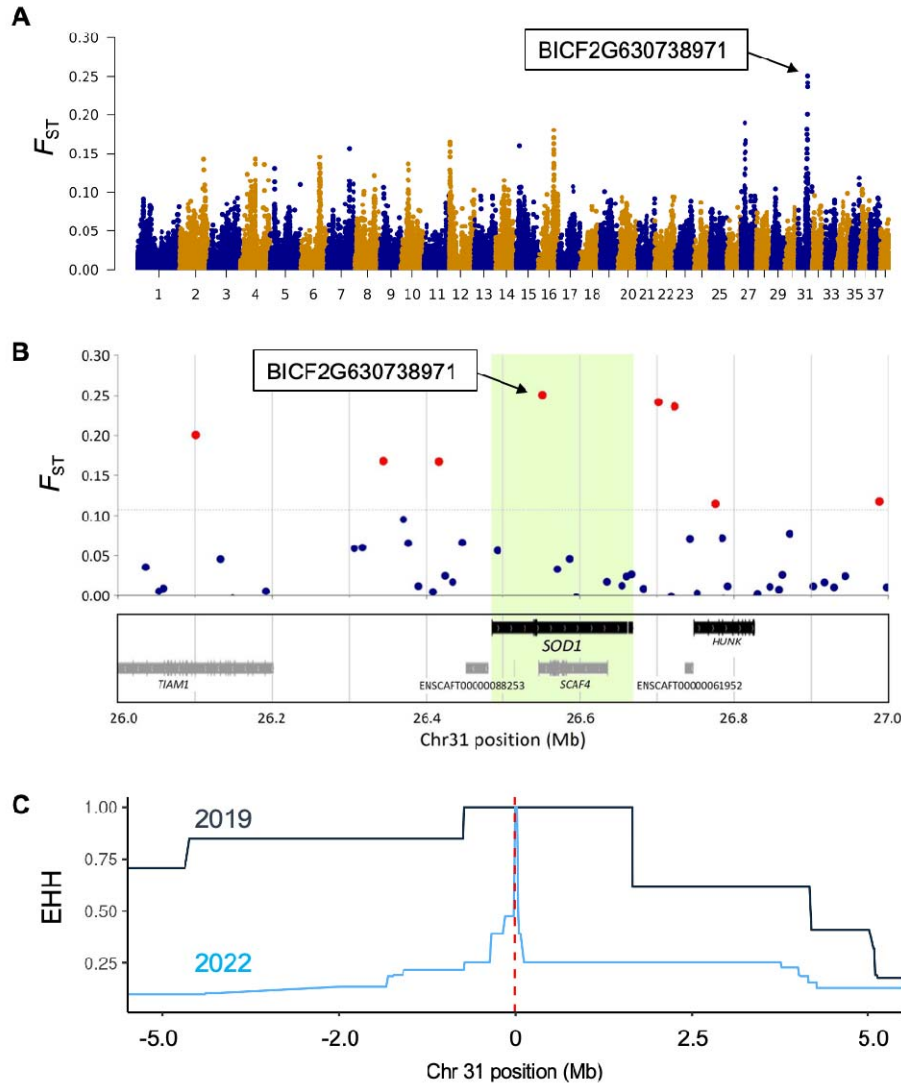
130 To further investigate the allele frequency of the *SOD1*: c.118G<A mutation, we
131 performed a simulation based on random genetic drift (10,000 replicates) for two models (i.e.,
132 scenarios where effective population sizes (N_e), which refers to the number of bred dogs, were
133 larger ($N_e = 540$) or smaller ($N_e = 49$); see Methods for details). Deviation from genetic drift
134 would indicate selection. The observed allele frequency was significantly lower than the simulated
135 one after 2018 in both models ($P < 0.05$; Fig. 1B, Table S1).

136

137 ***Selection signature***

138 To reveal the existence of selection signatures for *SOD1* and other regions at the
139 genome-wide level, we compared the 2019 and 2022 groups to determine the selection signature
140 in the PWC genome. Genome-wide SNP-based analyses on 117 PWC pups were performed
141 after determining their genetic backgrounds and separating them into four groups according to
142 the *SOD1*: c.118G<A genotype (Table S2). We set the Weir and Cockerham population
143 differentiation (F_{ST}) and simulation-based thresholds, and all SNPs with the top 0.1% F_{ST} values
144 met the simulation-based thresholds (Table S3; see Methods for details). Using both thresholds,
145 we selected 5 SNPs and identified 138 SNPs as candidates for selection (Table S3). The SNP
146 "BICF2G630738971" had the highest F_{ST} (0.25) of the 143,013 tested SNPs, and this SNP was
147 located in the intron of *SOD1* on canine chromosome 31 (Fig. 2A, B), 10,529 bp downstream of

148 *SOD1*: c.118G>A. We then calculated the extended haplotype homozygosity (EHH) of each
149 population (2019 vs. 2022) for BICF2G630738971 (Fig. 2C). The 2019 group had longer EHH
150 haplotypes than the 2022 group, although the position of *SOD1*: c.118G>A was closely linked to
151 the top SNP in the 2022 group ($0.47 < \text{EHH} < 1$).



152

153 **Figure 2. Selection signature observed in *SOD1*.**

154 A: Manhattan plot based on F_{ST} . B: Relationships of F_{ST} per SNP and their locations around
155 *SOD1* on chromosome 31. SNP BICF2G630738971 had the highest F_{ST} value. Red dots indicate
156 SNPs that exceeded the threshold of 0.1% F_{ST} . C: EHH of each group from the top F_{ST} SNP

157 (BICF2G630738971) for the derived allele. Dark-blue and light-blue lines indicate the 2019 and
158 2022 groups, respectively. The red dotted line indicates the position of *SOD1*: c.118G.

159

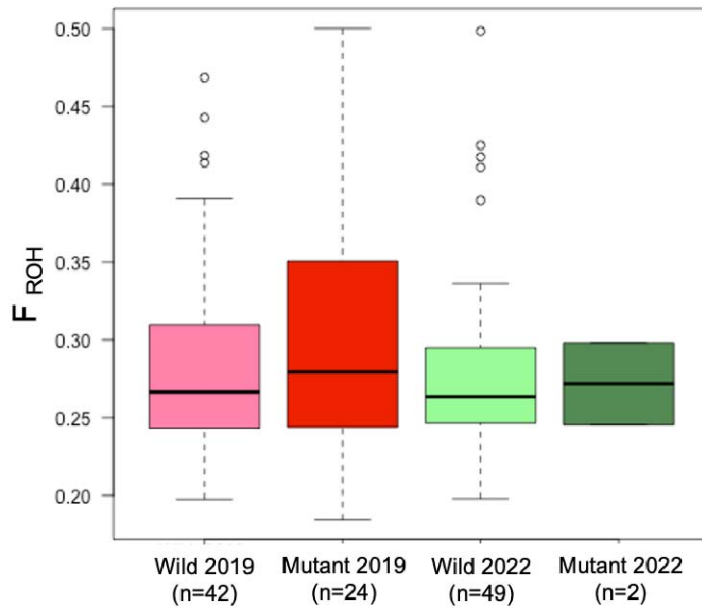
160 To investigate any other genes under selective pressure in addition to *SOD1*, we
161 surveyed the 186 genes that were included in or near the selected or candidate SNPs for
162 selection (Table S4). Four protein-coding genes (*ABCA4*, *TNXB*, *COL11A2*, and *SOD1*) reported
163 to affect phenotypes were identified (Fig. S1, Table S4). Gene Ontology (GO) analysis revealed
164 three significantly enriched terms (Fig. S2 and Table S5); one was related to peptide antigen
165 binding, and the others were related to the major histocompatibility complex (MHC).

166

167 ***Inbreeding levels and genetic structure***

168 We assessed inbreeding levels in the dog population. Observed heterozygosity (H_o) per group
169 was calculated using 142,510 SNPs; the H_o was 0.305 and 0.306 for the Wild 2019 and Wild
170 2022 groups, respectively. For mutant PWCs, the H_o was 0.296 and 0.314 in 2019 and 2022,
171 respectively. We then compared the inbreeding coefficients between groups based on runs of
172 homozygosity (F_{ROH}) (Fig. 3). The mean F_{ROH} was 0.29 ± 0.067 (standard deviation), $0.30 \pm$
173 0.082 , 0.28 ± 0.061 , and 0.27 ± 0.038 for Wild 2019, Mutant 2019, Wild 2022, and Mutant 2022
174 groups, respectively. The four groups did not differ significantly regarding inbreeding estimates
175 (Table S6).

176



177

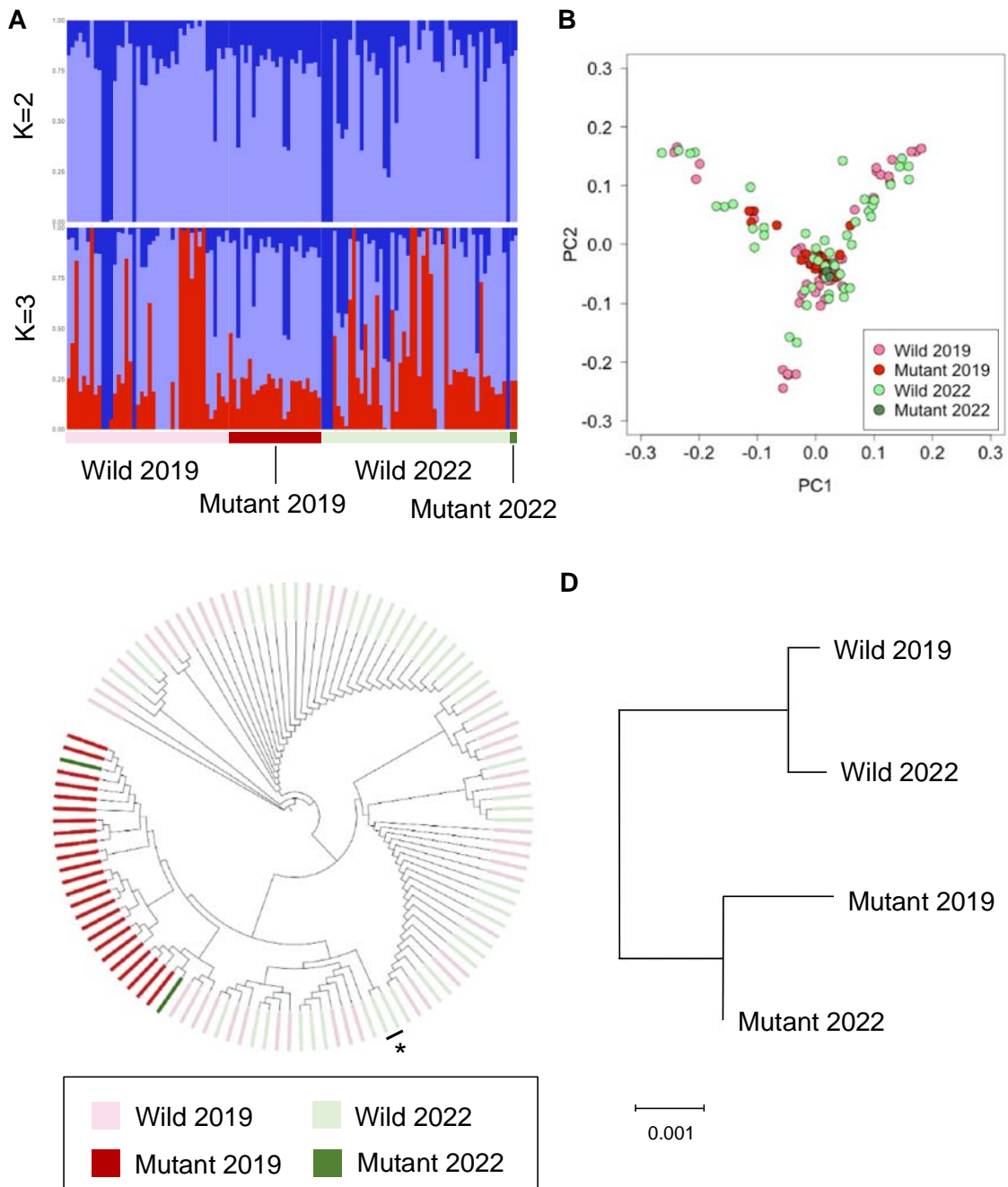
178 **Figure 3. Inbreeding estimates based on F_{ROH} and genome-wide SNP data.**

179 No significant difference was observed between populations (Welch's t-test, $P > 0.05$).

180

181 We analyzed the genetic structure through clustering using ADMIXTURE (Alexander et
182 al. 2009) and principal component analysis (PCA). Clustering results showed that the cross-
183 validation error was lowest when $K = 3$ (Fig. S3), with no obvious structure in the model with $K =$
184 3 (Fig. 4A). Likewise, PCA did not identify any obvious components that explained variation in the
185 dogs (Fig. 4B).

186



187

188 **Figure 4. Genetic structure and relatedness of PWCs.**

189 A: ADMIXTURE. B: PCA. C: Neighbor-joining phylogenetic tree. The asterisk of a lineage
190 includes only PWCs tested in 2022, indicating the dogs from different lineages in the 2019 group.
191 D: Dendrogram based on Nei's genetic distance.
192

193 We applied the neighbor-joining method for each PWC and Nei's genetic distance to infer
194 genetic relationships between groups. The phylogenetic tree revealed one clade that included all
195 Mutant dogs and another clade including all Wild dogs (Fig. 4C). The population-based Nei's
196 genetic distance indicated genetic similarities within the Mutant groups and within the Wild groups
197 (Fig. 4D). Both analyses revealed that PWCs homozygous for the *SOD1* mutation were more
198 common in certain lineages.

199 To estimate the potential number of dogs bred, we used the linkage disequilibrium
200 method to determine the contemporary *Ne* (Do et al. 2014). The contemporary *Ne* of Wild 2019 (*n*
201 = 42) was 48.9, lower than that of Wild 2022 (73.1, *n* = 49).

202

203 **Discussion**

204

205 Our analysis revealed that the availability of DTC genetic testing coincided with a decrease in the
206 frequency of homozygous *SOD1*: c.118G<A mutation among PWCs, reflecting negative selection
207 against the mutation. Our study provides valuable empirical evidence that genetic testing coupled
208 with selective breeding can lower mutation frequency in the span of a few years. With the
209 widespread, global availability of commercial genetic testing for *SOD1* mutations (Neeves and
210 Granger 2015), breeding programs can apply the test results and make informed systematic mate
211 selection decisions to decrease the frequency of this deleterious variant.

212 Genetic testing for adults and puppies started in 2017 and 2019, respectively. In this
213 study, the simulation, encompassing both large and small models, revealed a significant
214 decrease in the allele frequency of the mutation between 2017 and 2018. In addition, *F_{ST}* analysis
215 and the simulations suggested a strong selective pressure on the mutation between 2019 and

216 2022. These results indicate that genetic testing for adults and puppies has led to a decrease in
217 the frequency of the mutation. This decrease could be attributed to the introduction of large-scale
218 genetic testing for dogs by Japanese pet shops and breeders since 2017. Subsequently,
219 breeders may have avoided mating parents carrying the mutation. This prevented the production
220 of puppies with the mutation and continuously reduced its frequency between 2017 and 2022.

221 Studies investigating selection signatures during dog domestication (Akey et al. 2010;
222 Wang et al. 2013; Plassais et al. 2019) have identified an influence on phenotypes such as body
223 size, coat color, and behavior. To date, selection scans have mainly focused on a given region
224 over 10,000 years or similarly long periods (Akey et al. 2010). In contrast, selection scans over
225 short periods (a few years) in mammals are rare. Therefore, our results provide insights into the
226 genome evolution of mammals.

227 EHH is a widely used statistic in genome biology and evolutionary genetics to detect
228 regions of recent or ongoing positive selection (Sabeti et al. 2002). This statistic quantifies a
229 haplotype that quickly sweeps toward fixation, making it effective for detecting hard selective
230 sweeps. Theoretically, this observation can be detected in populations with random mating;
231 however, our study revealed longer haplotypes in the *SOD1* region in the 2019 group, as
232 opposed to the 2022 group, where a strong selection occurred. A potential reason for the shorter
233 haplotypes in the 2022 group could be genotype-based selection, employing breeds among a
234 larger number of dogs from multiple lineages. First, given that PWCs are inbred breeds, the
235 longer haplotypes observed in the 2019 group could be considered normal and not indicative of
236 selection. Over the course of three years, our SNP-based N_e estimation suggests that
237 approximately 1.5 times more dogs have been introduced and bred. Different lineages are
238 employed during mating to prevent pairing with dogs carrying the DM mutation, a practice
239 substantiated by our genetic analyses. Based on the genetic testing results, breeders mate dogs
240 without the mutation, leading to a high number of recombinations around the mutation site. Future
241 research, potentially employing model-based and/or observation-based approaches, will be
242 required to address this possibility.

243 While previous studies have focused on phenotype-driven selection, our current study
244 focuses on genotype-driven selection. Our results indicate that selective breeding was based on
245 the *SOD1* mutation, which causes canine DM. Here, in addition to *SOD1*, we identified three
246 candidate genes for selection (*ABCA4*, *TNXB*, and *COL11A2*) that have been reported to be
247 associated with disease phenotypes. *ABCA4* is associated with an autosomal recessive retinal
248 degenerative disease in Labrador retrievers (Mäkeläinen et al. 2019). Whole-genome sequencing
249 of mixed-breed dogs has revealed two missense variants in *TNXB*, which caused an Ehlers-
250 Danlos syndrome-like signature (Bauer et al. 2019). Additionally, the missense variant of
251 *COL11A2* is associated with skeletal dysplasia 2 and is inherited as a monogenic autosomal
252 recessive trait with incomplete penetrance, primarily in Labrador retrievers (Frischknecht et al.
253 2013). These genes may be associated with *SOD1* or DM while also being linked to valuable
254 traits beneficial for individual survival and/or breeding performance. Since our study revealed
255 selection signatures based on F_{ST} and genetic drift simulations, further research is essential to
256 identify selective pressure and the genes involved. This study also had a limitation. Unknown
257 admixture from other lineages may have introduced threshold bias, specifically for simulation-
258 based thresholds. For example, we detected a migration signature in the minor alleles of two
259 SNPs (BICF2G630168514 and BICF2G630168527, see Table S3), which were detected in the
260 2022 group but not in the 2019 group. This might be attributed to admixture from other lineages
261 identified in the 2022 group, as indicated by our population and phylogenetic analyses. The
262 simulation model employed here assumed a constant N_e , although our results indicate that
263 breeding size possibly increased between 2019 and 2022. Therefore, unknown admixture events
264 and fluctuations in breeding size were not factored in, potentially leading to an underestimation of
265 the threshold.

266 The MHC plays a central role in pathogen resistance (Debenham et al. 2005). Canine
267 MHC, also referred to as dog leukocyte antigen, exhibits genetic variations (Kennedy et al. 2007;
268 Niskanen et al. 2013) that are associated with autoimmune diseases (Jokinen et al. 2011;
269 Gershony et al. 2019). In this study, we found two GO terms related to the MHC for candidate

270 SNPs for selection. Considering that these terms were identified from the test results of pups, our
271 findings imply that selective pressure on the MHC region was related to survival in pups but not in
272 adults, possibly because the kennel environment necessitated the rapid development of a strong
273 pathogen-resistant autoimmune system. Evidence of post-copulatory selection at MHC-related
274 loci in puppies supports this hypothesis (Niskanen et al. 2016). However, we did not sequence
275 MHC haplotypes or obtain relevant phenotypes for each dog (e.g., survival rate). Thus, further
276 research is required to identify the mechanisms (e.g., targeting haplotypes) underlying MHC
277 selection.

278 Our research also demonstrated that the mutation can be selected against without
279 lowering the N_e (i.e., generating inbred animals). Inbreeding avoidance is essential for effective
280 animal breeding (Sams and Boyko 2019). Our genetic analysis revealed no differences in H_o and
281 inbreeding levels between the 2019 and 2022 groups. In addition, we estimated a larger N_e for
282 the 2022 group (73.1) than for the 2019 group (48.9). The phylogenetic analysis (Fig. 4C) further
283 implied that the genetic origin of some Wild dogs in 2022 was from other lineages. Taken
284 together, our findings suggest that PWC breeders used genetic testing results to limit inbreeding
285 while mating dogs from different families or lineages.

286 Notably, our study focused on the genotype of the *SOD1* mutation rather than the
287 phenotype. The median onset of DM in PWCs is 11 years (Coates et al. 2007). Considering the
288 start of DTC genetic testing in PWCs in Japan, the corresponding decreases in the prevalence of
289 *SOD1*-associated disease should be noticeable around the 2030s. Accordingly, further research
290 using comprehensive phenotypic datasets, such as those available from pet insurance
291 companies, is required to monitor DM onset in PWCs.

292 In conclusion, this study highlights the value of genetic testing as a tool to lower the risk
293 of canine DM while avoiding animal inbreeding. We conducted a genome-wide analysis of short-
294 term selection in PWCs and found that only a few years were required to reduce the number of
295 dogs homozygous for the mutant allele. Our results highlight that genetic testing could reduce the
296 prevalence of predictable genetic conditions, thus contributing to improved animal welfare.

297

298 **Materials and Methods**

299

300 ***Ethics statement***

301 We obtained all swab samples from dogs with the consent of their owners. The ethics
302 committee at the Anicom Specialty Medical Institute approved the study procedures (ID:2022-01).

303

304 ***Genotyping for the SOD1:c.118G<A variant and statistical testing***

305 Buccal swabs from 5,512 PWCs were sampled by breeders/owners and pet stores from
306 all over Japan between January 1, 2017, and December 31, 2022, with their consent. DNA was
307 extracted from oral mucosal tissue using a commercial kit (chemagic™ DNA Buccal Swab Kit,
308 PerkinElmer and DNAdvance Kit, Beckman Coulter). We performed real-time PCR to determine
309 genotypes of DM-associated mutations (*SOD1:c.118G<A*), specifically wild-type homozygotes
310 (G/G), heterozygous carriers (G/A), and variant homozygotes (A/A), as previously reported (Zeng
311 et al. 2014).

312 We used Fisher's exact test in R to compare the decrease in diploid genotypes between
313 2016 and 2022 (RCore 2016). Next, we employed the DriftSimulator.R in R to simulate allele
314 frequencies under genetic drift (<https://www.uni-goettingen.de/de/software/613074.html>). Given
315 the commencement of large-scale genetic testing in 2017, we used data from the previous year
316 (2016) for the simulation. Considering the difficulties in accurately inferring N_e , two genetic
317 models were considered in this study. The first, a large model, was based on the understanding
318 that approximately 10% of dogs sold annually in Japan are used for breeding
319 (https://www.env.go.jp/nature/dobutsu/aigo/2_data/pamph/rep_h1503.html). Thus, 540 dogs were
320 set as the N_e for 2016, given that 5,395 PWCs had been registered with the Japan Kennel Club
321 (<https://www.jkc.or.jp/archives/enrollment/4598>). The second, a small model, was estimated
322 based on the SNPs in this study (see Estimating N_e section) and was set at 49. The breeding
323 cycle was set as one per year, indicating that six breeding generations had passed over six years

324 (2016–2022). The sex ratio was set at 20% for males and 80% for females. Using these
325 parameters, we conducted 10,000 simulations of genetic drift (simulated allele frequency) and
326 adopted the resultant distribution as the null for subsequent comparisons with observed allele
327 frequencies through six years. Next, we calculated the 95% confidence interval of the observed
328 allele frequency based on a binomial distribution using the *binom.test* function implemented in R.
329 Furthermore, we calculated the probability of the observed allele frequency being lower than that
330 of the simulated allele frequencies. The probability was determined by dividing the number of
331 simulated allele frequencies lower than the observed frequency by 10,000. Significance was set
332 at $P < 0.05$ for both tests.

333

334 ***Genome-wide SNP genotyping***

335 We used an SNP-genotyping array (Canine 230 K Consortium BeadChip Array, Illumina,
336 San Diego, CA, USA) to investigate the effects of genetic testing on the whole genome. We
337 compared genome-wide SNPs from four subpopulations of wild-type and variant homozygotes of
338 the *SOD1* risk allele, all derived from dogs born in 2019 and 2022. Considering the effect of
339 genetic background on array-based analyses, we selected all dogs from the two largest clients for
340 array-based analyses (Table S1). We used an SNP-genotyping array (Canine 230 K consortium)
341 and the Illumina iScan system to detect over 230 K SNP genotypes. Genotype coordinates
342 corresponded to the CanFam3.1 genome assembly.

343 We conducted quality control using PLINK version 1.90 (Chang et al. 2015). Missing
344 rates for each locus (geno option) and individual dogs (mind option) were both $< 1\%$. We did not
345 examine the Hardy-Weinberg equilibrium as we did not assume random mating for pedigree
346 PWC. Population genetic analyses should not include close relatives; therefore, we conducted
347 robust relationship-based pruning (Manichaikul et al. 2010) using the king-cutoff option in PLINK
348 version 2.00a2LM, with a threshold of 0.176 to exclude pairings between monozygotic twins and
349 first-degree relatives. For allele frequency-based quality control, we excluded SNPs with a minor
350 allele frequency of < 0.01 . We also removed sex chromosome variants and autosomal indels

351 (insertions-deletions) because their effects on allele frequency differ from those of autosomal
352 SNPs. The final analysis retained 143,013 SNPs. After quality control for individual dogs,
353 including the removal of related animals, 117 dogs remained: homozygous wild-type (G/G) dogs
354 tested in 2019 (Wild 2019, n = 42) and in 2022 (Wild 2022, n = 49) as well as homozygous
355 mutant dogs tested in 2019 (Mutant 2019, n = 24) and in 2022 (Mutant 2022, n = 2; Table S2).
356 We employed this dataset for subsequent analyses.

357

358 ***Detecting selection pressure on SNPs***

359 Artificial selection alters the frequency of genes associated with phenotypes. To identify
360 selection signatures in the PWC genome, we estimated F_{ST} in the 2019 and 2022 groups. We
361 estimated F_{ST} values using the –fst option implemented in PLINK version 1.9. The first threshold
362 for selective pressure was based on SNPs with F_{ST} values in the upper 0.1%. In addition to the
363 F_{ST} -based scan, we conducted a more rigorous detection using a simulation-based scan. We also
364 implemented a simulation based on genetic drift, conducting it 10,000 times. The small model (N_e
365 = 49) was used to assign a rank, indicating the probability of frequency to increase/decrease in
366 2022 compared to that in 2019. Subsequently, we set the second threshold to below 0.025 (rank
367 250) or above 0.975 (rank 9750; two-sided 2.5 percentile) as the suggestive level and performed
368 additional Bonferroni correction for 143 SNPs below 0.001 (rank 1) or above 0.999 (rank 9999;
369 two-sided 1.7 percentile) as the significant level. The SNPs that met the criteria of the first
370 threshold were subjected to the simulation-based scan. The SNPs that passed the suggestive
371 level were denoted as “candidate SNPs for selection” and those that passed the significant level
372 were denoted as “selected SNPs”. Genes in the \pm 100 kb region surrounding SNPs which passed
373 thresholds with suggestive and significant level were considered candidate selected genes.

374 Furthermore, to investigate haplotype length surrounding *SOD1* mutation, we calculated
375 the EHH of wild-type populations. The EHH is a measure used to detect genome regions under
376 recent selective pressure (Sabeti et al. 2002). First, target SNPs under selective pressure in the
377 Wild 2019 and 2022 populations were phased using Beagle 5.4 (version 22Jul22.46e) (Browning

378 et al. 2018) with default settings. After phasing, EHH for the target SNP was estimated using a 1
379 Mbp window in SelScan version 2.0.0 (Szpiech and Hernandez 2014).

380 To determine the functional classes of genes associated with the analyzed traits, we
381 performed a GO analysis powered by PANTHER (Thomas et al. 2022). We selected target genes
382 using linkage disequilibrium analysis and the PANTHER overrepresentation test (release
383 20221013). ‘Molecular function’ was used for domestic dog (*Canis lupus familiaris*) dataset
384 annotation in PANTHER 17.0. Ensembl gene IDs were used for data annotation. Statistical
385 differences were assessed using Fisher’s exact test. A false discovery rate of $P < 0.05$ was
386 considered significant.

387 We obtained all gene datasets from the Ensembl Genome Browser (release 104;
388 CanFam 3.1) and retrieved Ensembl gene IDs using Bedtools version 2.27.1 (Quinlan and Hall
389 2010; Danecek et al. 2021).

390

391 ***Inbreeding levels***

392 We inferred inbreeding levels using specimens from genome-wide SNP genotyping. The
393 R package DetectRuns was used to obtain the proportion of times each SNP fell inside a run per
394 population, corresponding to locus homozygosity or heterozygosity in the respective population.
395 We used the following DetectRuns parameters: minSNP = 41, maxGap 10^6 , minLengthBps =
396 50000, and minDensity = 1/5000.

397

398 ***Population genetics***

399 To clarify the genetic structure and phylogenetic relationships in the PWC population, we
400 performed PCA using PLINK version 1.9 with default settings and maximum-likelihood ancestry
401 analysis using ADMIXTURE version 1.3 (Alexander et al. 2009). For ADMIXTURE, we set the
402 number of populations (K) between 2 and 10. We used the option cv for cross-validation error
403 calculation to select the optimal K value based on the lowest error.

404 For genetic relationships, we first converted the PLINK PED format into FASTA format.

405 We then converted the FASTA file to NEXUS format in MEGA X (Kumar et al. 2018). We
406 constructed a phylogenetic tree using the neighbor-joining algorithm with p-distance in MEGA X.

407 We calculated Nei's standard genetic distance D (Nei 1987) between the four populations
408 (Wild 2019, Wild 2022, Mutant 2019, and Mutant 2022). Nei's D was estimated using GenoDive
409 version 3.06 with default settings (Meirmans and Van Amsterdam 2019).

410

411 ***Estimating Ne***

412 The contemporary *Ne* of PWC was estimated from genome-wide SNP data using a
413 linkage disequilibrium method in NeEstimator version 2.1 (Do et al. 2014). The lowest allele
414 frequency was set at 0.01.

415

416 **Data availability**

417 SNP data for the PWCs are available from the Dryad database (DOI: 10.5061/dryad.rbnzs7hhk)
418

419 **Acknowledgments**

420 We thank all participating breeders, veterinarians, and dog owners for collecting buccal swabs
421 from their dogs. We also thank Dr. Ryo Horie, Mr. Ryuta Kuwana, and all the Anicom Specialty
422 Medical Institute members for their feedback on this study. This study was supported by the
423 Research Foundation of Anicom Specialty Medical Institute.

424

425 **Author Contributions**

426 YM and HU designed the study; HU, NA, FY, GI, KO, and YM collected dog samples, performed
427 experiments, contributed to the analytical tools, analyzed the data, and wrote the paper.

428

429 **Competing Interest Statement**

430 HU, FY, and KO received salaries from Anicom Pafe, a genetic testing company in Japan. NA,
431 GI, and YM received wages from Anicom Specialty Medical Institute. YM also received a stipend
432 from Azabu University.

433

434 **References**

435 Akey JM, Ruhe AL, Akey DT, Wong AK, Connelly CF, Madeoy J, Nicholas TJ, Neff MW. 2010.
436 Tracking footprints of artificial selection in the dog genome. *Proc. Natl. Acad. Sci. U. S. A.* 107:1160–1165.

437 Akiyama N, Suzuki R, Saito T, Yuchi Y, Ukawa H, Matsumoto Y. 2023. Presence of known feline
438 ALMS1 and MYBPC3 variants in a diverse cohort of cats with hypertrophic
439 cardiomyopathy in Japan. *PLoS One* 18:e0283433.

440 Alexander DH, Novembre J, Lange K. 2009. Fast model-based estimation of ancestry in
441 unrelated individuals. *Genome Res.* 19:1655–1664.

442 Awano T, Johnson GS, Wade CM, Katz ML, Johnson GC, Taylor JF, Perloski M, Biagi T,
443 Baranowska I, Long S, et al. 2009. Genome-wide association analysis reveals a SOD1
444 mutation in canine degenerative myelopathy that resembles amyotrophic lateral sclerosis.
445 *Proc. Natl. Acad. Sci. U. S. A.* 106:2794–2799.

446 Ayala-Valdovinos MA, Gomez-Fernandez A. 2018. Frequency of canine degenerative myelopathy
447 SOD1: c. 118G> A mutation in 22 dog breeds in Guadalajara, Mexico. *de Ciencias
448 Pecuarias* [Internet]. Available from: http://www.scielo.org.co/scielo.php?pid=S0120-06902018000200150&script=sci_arttext&tlang=en

449 Bauer A, de Lucia M, Leuthard F, Jagannathan V, Leeb T. 2019. Compound heterozygosity for
450 TNXB genetic variants in a mixed-breed dog with Ehlers-Danlos syndrome. *Anim. Genet.*
451 50:546–549.

452 Boyko AR, Boyko RH, Boyko CM, Parker HG, Castelhano M, Corey L, Degenhardt JD, Auton A,
453 Hedimbi M, Kityo R, et al. 2009. Complex population structure in African village dogs and
454 its implications for inferring dog domestication history. *Proc. Natl. Acad. Sci. U. S. A.*
455 106:13903–13908.

456 Browning BL, Zhou Y, Browning SR. 2018. A One-Penny Imputed Genome from Next-Generation
457 Reference Panels. *Am. J. Hum. Genet.* 103:338–348.

458 Chang CC, Chow CC, Tellier LC, Vattikuti S, Purcell SM, Lee JJ. 2015. Second-generation
459 PLINK: rising to the challenge of larger and richer datasets. *Gigascience* 4:7.

460 Chang H-S, Kamishina H, Mizukami K, Momoi Y, Katayama M, Rahman MM, Uddin MM, Yabuki
461 A, Kohyama M, Yamato O. 2013. Genotyping assays for the canine degenerative
462 myelopathy-associated c.118G>A (p.E40K) mutation of the SOD1 gene using
463 conventional and real-time PCR methods: a high prevalence in the Pembroke Welsh
464 Corgi breed in Japan. *J. Vet. Med. Sci.* 75:795–798.

465 Chu ET, Simpson MJ, Diehl K, Page RL, Sams AJ, Boyko AR. 2019. Inbreeding depression
466 causes reduced fecundity in Golden Retrievers. *Mamm. Genome* 30:166–172.

467 Coates JR, March PA, Oglesbee M, Ruaux CG, Olby NJ, Berghaus RD, O'Brien DP, Keating JH,
468 Johnson GS, Williams DA. 2007. Clinical characterization of a familial degenerative
469 myelopathy in Pembroke Welsh Corgi dogs. *J. Vet. Intern. Med.* 21:1323–1331.

470 Danecek P, Bonfield JK, Liddle J, Marshall J, Ohan V, Pollard MO, Whitwham A, Keane T,
471 McCarthy SA, Davies RM, et al. 2021. Twelve years of SAMtools and BCFtools.
472 *Gigascience* 10:giab008.

473 Debenham SL, Hart EA, Ashurst JL, Howe KL, Quail MA, Ollier WER, Binns MM. 2005. Genomic
474 sequence of the class II region of the canine MHC: comparison with the MHC of other
475 mammalian species. *Genomics* 85:48–59.

478 Do C, Waples RS, Peel D, Macbeth GM, Tillett BJ, Ovenden JR. 2014. NeEstimator v2: re-
479 implementation of software for the estimation of contemporary effective population size
480 (Ne) from genetic data. *Mol. Ecol. Resour.* 14:209–214.

481 Dreger DL, Hooser BN, Hughes AM, Ganesan B, Donner J, Anderson H, Holtvoigt L, Ekenstedt
482 KJ. 2019. True Colors: Commercially-acquired morphological genotypes reveal hidden
483 allele variation among dog breeds, informing both trait ancestry and breed potential.
484 *PLoS One.* 14:e0223995.

485 Dreger DL, Rimbault M, Davis BW, Bhatnagar A, Parker HG, Ostrander EA. 2016. Whole-
486 genome sequence, SNP chips and pedigree structure: building demographic profiles in
487 domestic dog breeds to optimize genetic-trait mapping. *Dis. Model. Mech.* 9:1445–1460.

488 Frischknecht M, Niehof-Oellers H, Jagannathan V, Owczarek-Lipska M, Drögemüller C, Dietschi
489 E, Dolf G, Tellhelm B, Lang J, Tiira K, et al. 2013. A COL11A2 mutation in Labrador
490 retrievers with mild disproportionate dwarfism. *PLoS One* 8:e60149.

491 Gershony LC, Belanger JM, Short AD, Le M, Hytönen MK, Lohi H, Famula TR, Kennedy LJ,
492 Oberbauer AM. 2019. DLA class II risk haplotypes for autoimmune diseases in the
493 bearded collie offer insight to autoimmunity signatures across dog breeds. *Canine Genet.
Epidemiol.* 6:2.

494 Jokinen P, Rusanen EM, Kennedy LJ, Lohi H. 2011. MHC class II risk haplotype associated with
495 canine chronic superficial keratitis in German Shepherd dogs. *Vet. Immunol.
Immunopathol.* 140:37–41.

496 Kawakami T, Raghavan V, Ruhe AL, Jensen MK, Milano A, Nelson TC, Boyko AR. 2022. Early
497 onset adult deafness in the Rhodesian Ridgeback dog is associated with an in-frame
500 deletion in the EPS8L2 gene. *PLoS One* 17:e0264365.

501 Kennedy LJ, Barnes A, Short A, Brown JJ, Lester S, Seddon J, Fleeman L, Francino O, Brkljacic
502 M, Knyazev S, et al. 2007. Canine DLA diversity: 1. New alleles and haplotypes. *Tissue
503 Antigens* 69 Suppl 1:272–288.

504 Kumar S, Stecher G, Li M, Knyaz C, Tamura K. 2018. MEGA X: Molecular Evolutionary Genetics
505 Analysis across Computing Platforms. *Mol. Biol. Evol.* 35:1547–1549.

506 Lindblad-Toh K, Wade CM, Mikkelsen TS, Karlsson EK, Jaffe DB, Kamal M, Clamp M, Chang JL,
507 Kulbokas EJ 3rd, Zody MC, et al. 2005. Genome sequence, comparative analysis and
508 haplotype structure of the domestic dog. *Nature* 438:803–819.

509 Mäkeläinen S, Gödia M, Hellsand M, Viluma A, Hahn D, Makdoumi K, Zeiss CJ, Mellersh C,
510 Ricketts SL, Narfström K, et al. 2019. An ABCA4 loss-of-function mutation causes a
511 canine form of Stargardt disease. *PLoS Genet.* 15:e1007873.

512 Manichaikul A, Mychaleckyj JC, Rich SS, Daly K, Sale M, Chen W-M. 2010. Robust relationship
513 inference in genome-wide association studies. *Bioinformatics* 26:2867–2873.

514 Meirmans P, Van Amsterdam I. 2019. GenoDive. Available from:
515 <http://www.bentleydrummer.nl/software/GenoDiveManual.pdf>

516 Mellanby RJ, Ogden R, Clements DN, French AT, Gow AG, Powell R, Corcoran B, Schoeman
517 JP, Summers KM. 2013. Population structure and genetic heterogeneity in popular dog
518 breeds in the UK. *Vet. J.* 196:92–97.

519 Moses L, Niemi S, Karlsson E. 2018. Pet genomics medicine runs wild. *Nature* 559:470–472.

520 Neeves J, Granger N. 2015. An update on degenerative myelopathy in dogs. *Compan. Anim.*
521 20:408–412.

522 Nei M. 1987. Molecular Evolutionary Genetics. Columbia University Press

523 Niskanen AK, Hagström E, Lohi H, Ruokonen M, Esparza-Salas R, Aspi J, Savolainen P. 2013.
524 MHC variability supports dog domestication from a large number of wolves: high diversity
525 in Asia. *Heredity* 110:80–85.

526 Niskanen AK, Kennedy LJ, Lohi H, Aspi J, Pyhäjärvi T. 2016. No evidence of prenatal diversifying
527 selection at locus or supertype levels in the dog MHC class II loci. *Canine Genet.
Epidemiol.* 3:9.

528 Plassais J, Kim J, Davis BW, Karyadi DM, Hogan AN, Harris AC, Decker B, Parker HG,
529 Ostrander EA. 2019. Whole genome sequencing of canids reveals genomic regions
530 under selection and variants influencing morphology. *Nat. Commun.* 10:1489.

531

532 Quinlan AR, Hall IM. 2010. BEDTools: a flexible suite of utilities for comparing genomic features.
533 *Bioinformatics* 26:841–842.

534 RCore Team. 2016. R: A language and environment for statistical computing. R Foundation for
535 Statistical Computing, Vienna, Austria.

536 Rokhsar JL, Canino J, Raj K, Yuhnke S, Slutsky J, Giger U. 2021. Web resource on available
537 DNA variant tests for hereditary diseases and genetic predispositions in dogs and cats:
538 An Update. *Hum. Genet.* 140:1505–1515.

539 Sabeti PC, Reich DE, Higgins JM, Levine HZP, Richter DJ, Schaffner SF, Gabriel SB, Platko JV,
540 Patterson NJ, McDonald GJ, et al. 2002. Detecting recent positive selection in the human
541 genome from haplotype structure. *Nature* 419:832–837.

542 Sams AJ, Boyko AR. 2019. Fine-Scale Resolution of Runs of Homozygosity Reveal Patterns of
543 Inbreeding and Substantial Overlap with Recessive Disease Genotypes in Domestic
544 Dogs. *G3 (Bethesda)* 9:117–123.

545 Szpiech ZA, Hernandez RD. 2014. selscan: An Efficient Multithreaded Program to Perform EHH-
546 Based Scans for Positive Selection. *Mol. Biol. Evol.* 31:2824–2827.

547 Thomas PD, Ebert D, Muruganujan A, Mushayahama T, Albou L-P, Mi H. 2022. PANTHER:
548 Making genome-scale phylogenetics accessible to all. *Protein Sci.* 31:8–22.

549 Wang G-D, Zhai W, Yang H-C, Fan R-X, Cao X, Zhong L, Wang L, Liu F, Wu H, Cheng L-G, et
550 al. 2013. The genomics of selection in dogs and the parallel evolution between dogs and
551 humans. *Nat. Commun.* 4:1860.

552 Zeng R, Coates JR, Johnson GC, Hansen L, Awano T, Kolicheski A, Ivansson E, Perloski M,
553 Lindblad-Toh K, O'Brien DP, et al. 2014. Breed Distribution of *SOD 1* Alleles Previously
554 Associated with Canine Degenerative Myelopathy. *J. Vet. Intern. Med.* 28:515–521.